ARL-TR-77-46

LABORATORY AND IN SITU SEDIMENT ACOUSTICS

Summary Report under Contract N00014-76-C-0117

Donald J. Shirley

APPLIED RESEARCH LABORATORIES
THE UNIVERSITY OF TEXAS AT AUSTIN
POST OFFICE BOX 8029, AUSTIN, TEXAS 78712

23 August 1977

Summary Report

1 September 1975 - 31 December 1976

D D C
OCT 19 1977
C

Prepared for

OFFICE OF NAVAL RESEARCH
DEPARTMENT OF THE NAVY
ARLINGTON, VA 22217

REPORT DOCUMENTATION PAGE	READ INSTRUCTIONS BEFORE COMPLETING FORM

1. REPORT NUMBER	2. GOVT ACCESSION NO.	3. RECIPIENT'S CATALOG NUMBER

4. TITLE (and Subtitle)	5. TYPE OF REPORT & PERIOD COVERED
LABORATORY AND IN SITU SEDIMENT ACOUSTICS.	summary report 1 Sep 75 — 31 Dec 76,
	6. PERFORMING ORG. REPORT NUMBER ARL-TR-77-46

7. AUTHOR(s)	8. CONTRACT OR GRANT NUMBER(s)
Donald J. Shirley	N00014-76-C-0117

9. PERFORMING ORGANIZATION NAME AND ADDRESS	10. PROGRAM ELEMENT, PROJECT, TASK AREA & WORK UNIT NUMBERS
Applied Research Laboratories The University of Texas at Austin Austin, Texas 78712	

11. CONTROLLING OFFICE NAME AND ADDRESS	12. REPORT DATE
Office of Naval Research Department of the Navy Arlington, Virginia 22217	23 Aug 77
	13. NUMBER OF PAGES 56

14. MONITORING AGENCY NAME & ADDRESS(if different from Controlling Office)	15. SECURITY CLASS. (of this report)
	UNCLASSIFIED
	15a. DECLASSIFICATION/DOWNGRADING SCHEDULE

16. DISTRIBUTION STATEMENT (of this Report)

Approved for public release; distribution unlimited.

17. DISTRIBUTION STATEMENT (of the abstract entered in Block 20, if different from Report)

18. SUPPLEMENTARY NOTES

19. KEY WORDS (Continue on reverse side if necessary and identify by block number)

compressional wave speed
shear wave speed
acoustic impedance
profilometer

20. ABSTRACT (Continue on reverse side if necessary and identify by block number)

During the period 1 September 1975 - 31 December 1976 work continued at ARL:UT on research directed at measuring sediment acoustic parameters in situ. Four field trips were made to use the ARL profilometer to make in situ sound speed measurements. Laboratory work continued to add the capability of measuring shear wave speed and acoustic impedance to the existing profilometer. Shear wave and compressional wave data measured in laboratory sediments are reported. (U)

DD FORM 1473 1 JAN 73   EDITION OF 1 NOV 65 IS OBSOLETE

TABLE OF CONTENTS

I. INTRODUCTION

During 1976 the work under Contract N00014-76-C-0117 was in three major areas. The first area was the utilization of the ARL:UT profilometer system that had previously been developed and built at Applied Research Laboratories, The University of Texas at Austin (ARL:UT) (Shirley et al., 1973; Shirley and Anderson, 1974). The profilometer system was used on four coring field trips conducted by three organizations, Woods Hole Oceanographic Institute (WHOI), Lamont-Doherty Geological Observatory of Columbia University (LDGO) and the Geophysics Laboratory of the Marine Science Institute, The University of Texas (MSI).

Work with WHOI included two field trips using the Woods Hole giant piston corer (GPC). No data were obtained on these trips because of profilometer malfunction and loss of the GPC with profilometer attached.

One trip was made to the North Atlantic south of Bermuda aboard R/V CONRAD operated by LDGO. Seven profiles were made during this trip with penetrations on all cores on the order of 13 m. However, problems with the coring winch reduced the amount of data gathered.

One field trip was conducted with MSI on R/V IDA GREEN during which 77 cores were taken in shallow water off the coast of Florida in the Gulf of Mexico. About 60 successful profiles were made out of 77 attempts during this coring operation.

Concurrent with the profilometer field trips, work was proceeding in the laboratory study of shear waves. Transducers capable of measuring shear waves in ocean bottom sediments have been developed at ARL:UT (Shirley and Anderson, 1975). Most of the work with shear waves was to refine the size and sensitivity of the shear wave transducers so

1

that the transducers could be incorporated in the ARL:UT profilometer to measure both shear and compressional acoustical properties simultaneously. As work progressed on the shear wave transducers, measurements were made on laboratory sediments, for two reasons. First, the capability of measuring both shear and compressional wave parameters in laboratory sediments would provide data points not previously obtainable and, second, laboratory measurements would provide a baseline for evaluating the new shear transducers, and would also expose problem areas in their use. This second aspect was a necessary adjunct to the shear transducer development.

Another effort this past year was the development of an acoustic transducer that would measure the bulk density of a sediment. It was shown previously that the acoustic impedance of a medium can be measured by measuring the electrical impedance of a driven transducer in contact with that medium (Shirley and Anderson, 1975). If measurements of compressional wave speed (C_p) could be made simultaneous with measurements of acoustic impedance (ρC_p), a measurement of bulk density (ρ) can be obtained with minimum disturbance to the sediment. Again, the development of the acoustic impedance measuring transducer was undertaken with the goal of incorporating it in the profilometer package.

The thrust of the program has been to develop an instrument capable of making concurrent measurements of compressional wave speed, shear wave speed, and bulk density in situ during normal coring procedures. If these three parameters are known, the elastic properties of a sediment can be calculated. Since signal amplitude can be obtained from the profilometer, compressional and shear attenuations can be measured, and thus the viscoelastic properties of the sediment calculated. However, up to now meaningful measurements have not been possible because the sensitivity of the profilometer to the relatively small acoustic attenuations encountered in ocean bottom sediments has been too low. This future refinement of the system will make possible an additional valuable measurement.

2

II. PROFILOMETER

The ARL:UT compressional wave profilometer is an instrument designed
and constructed to attach to existing coring equipment with a minimum
amount of modification to that equipment. Figure 1 shows the equipment
and how it is deployed on a corer. Electronic circuits, batteries, and a
cassette tape recorder are housed in an aluminum cylinder capable of
withstanding 6.9×10^4 kPa ambient pressure. The electronic package
is attached to the top, weighted end of the corer. Two transducers are
attached to the cutter at the bottom of the corer and are connected to
the electronic circuits through two armored electrical cables taped to
the outside of the core barrel. One transducer emits a 200 kHz pulse
and the opposite transducer receives; the measurement taken is the
travel time across the diameter of the corer between transducers. The
electronic package also includes an accelerometer to measure deceleration
of the corer, which can be integrated to produce a depth record.

The first compressional wave profilometer coring field trip for the
year was conducted during the period 4 August - 2 September 1975, in the
North Atlantic between Iceland and Scotland. The trip was made aboard
R/V KNORR operated by WHOI and used the WHOI giant piston corer. During
a previous shakedown cruise in June 1975, one of the corers had been
lost with one of the two ARL:UT profilometers aboard. Another GPC was
lost at the start of the August cruise, but without the profilometer
attached. After building another GPC aboard ship, the cruise was continued.
Four drops were made with the profilometer attached, but no profiles were
made because of several malfunctions in the profilometer electronic circuits.

The next field work with the profilometer was during a coring
expedition by Lamont-Doherty Geological Observatory personnel aboard

3

ELECTRONIC PACKAGE

ARMORED CABLE

CORER

TRANSDUCERS

FIGURE 1

ARL COMPRESSIONAL WAVE PROFILOMETER

4

0166(17)-8

R/V ROBERT CONRAD to the North Atlantic just south and west of Bermuda.
Areas that were cored included the West Bermuda Rise, Southwest Edge of
the Bermuda Rise, West Antilles Outer Ridge, and the Nares Abyssal Plain.
Eleven piston cores were taken of which nine were made with the profilom-
eter attached. No sound speed profile was obtained from the first two
cores owing to a malfunction of the coring winch, which resulted in the
time to reach the bottom exceeding the recording time of the profilometer.
The winch was repaired and seven successful profiles were made before
a major winch failure stopped the piston coring on this leg of the cruise.

Table I lists the seven profiled cores and their location and water
depth from the ship's precision depth recorder (PDR) records. As each
core was recovered and extruded, laboratory sound speed measurements
were made in increments along the core by LDGO personnel. The axis of
sound propagation for the laboratory measurements was parallel to the
length of the core, and 90° to the axis of propagation in the profilometer
measurements. As each sound speed measurement was made, the core was
sampled for physical properties measurements. This cruise was the
first time that shipboard laboratory sound speed profiles had been made
that could be compared to the in situ profiles from the ARL:UT profilometer.

Figure 2 shows the in situ sound speed profile for core RC19-14,
and Fig. 3 shows the signal amplitude profile for the same core. In
both profiles, the top of the sediment column lies to the left, and a
short segment of the overlying water is included at the far left. At
the sediment-water interface (zero on the depth axis) the sound speed
profile shows a decrease in sound speed. After this initial decrease
in sound speed, the gross profile shows a linearly increasing sound
speed with a great many sudden decreases in the profile. The amplitude
profile of Fig. 3 shows a sudden decrease in signal level as the trans-
ducers enter the sediment, indicating that the signal is no longer
sufficient to make a proper sound speed measurement. As the corer
penetrates further, there are many more sharp decreases in the amplitude

5

TABLE I

Core No.	Location	Latitude	Longitude	Depth (m)
RC19-14	Southwest Bermuda Rise	26° 10.3'N	69° 47.8'W	5263
RC19-15	West Antilles Outer Ridge	23° 54.7'N	68° 51.7'W	5232
RC19-17	West Antilles Outer Ridge	23° 53.3'N	68° 53.4'W	5207
RC19-18	West Antilles Outer Ridge	23° 54.1'N	68° 53.0'W	5221
RC19-20	Nares Abyssal Plain	22° 51.2'N	66° 13.0'W	5616
RC19-21	Nares Abyssal Plain	22° 51.8'N	66° 12.2'W	5616
RC19-22	Nares Abyssal Plain	22° 50.8'N	66° 18.6'W	5616
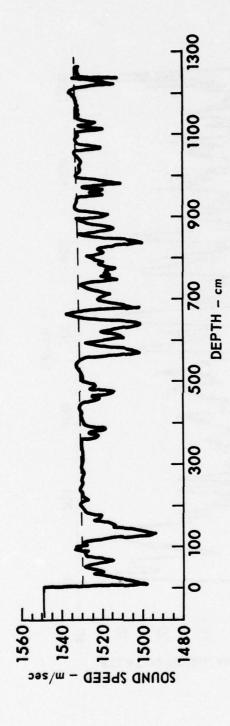
FIGURE 2

IN SITU SOUND SPEED PROFILE FOR CORE RC 19-14

7

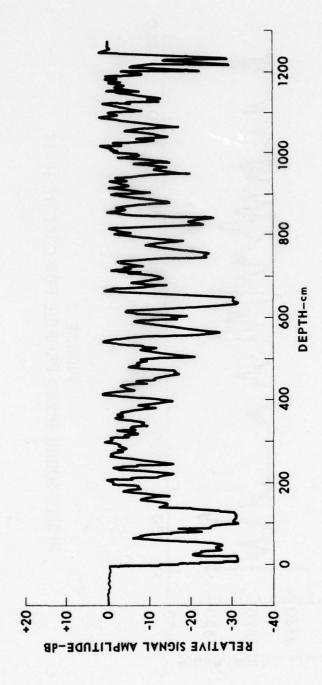FIGURE 3
IN SITU SIGNAL AMPLITUDE PROFILE FOR CORE RC 19-14

8

curve, and these decreases correlate directly with the decreases in the sound speed curve. This correlation indicates that the decreases in the sound speed profile are not actual changes in sediment sound speed but are rather points at which the signal level is too low to take measurements.

These data dropouts occur when the high sound speed layers in the sediment are of the same order of thickness as the width of the radiating face of the profilometer transducers. Sound traveling in the thin high speed layers mixes with sound traveling in the lower speed sediment on each side and this causes phase interference. If the relative phase is such as to reinforce the signal, no interference is produced, but if the mixing is destructive the amplitude can easily go below the 20 dB dynamic range of the instrument and causes a data dropout. In this profile the problem was aggravated by the plastic encapsulant of the transducer elements cracking under ambient pressure of the deep ocean. Since these same transducers had been used successfully (in 1974) at the same depths, it was felt that aging of the plastic was the cause of this malfunction. The cracking was not severe enough to destroy the transducers, but did impair their sensitivity so that excessive dropouts resulted (transducers have subsequently been built using a less rigid, more stable plastic).

Figure 4 is a laboratory sound speed profile of core RC19-14 made with data supplied by LDGO personnel. The dotted portion to the left of the profile shows the water sound speed calculated from depth and temperature data for the site. Although the data dropouts described above make direct comparisons difficult, the two profiles show similar behavior. It is of interest to note that the laboratory measurement is not sensitive to the effects of the thin high velocity layers. The major discrepancy between the two is a generally lower sound speed of about 10 m/sec indicated by the laboratory data.

Figures 5 through 7 show in situ sound speed profiles made for cores 15, 17, and 18 while Figs. 8 through 10 show the corresponding
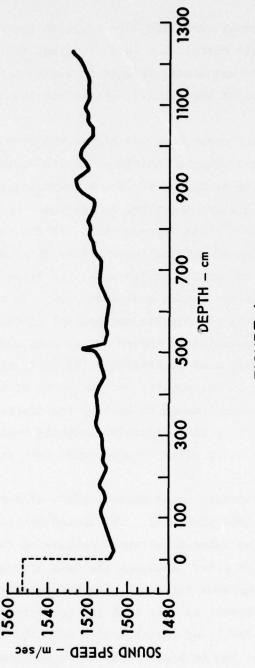
9

FIGURE 4

LABORATORY SOUND SPEED PROFILE FOR CORE RC 19 - 14
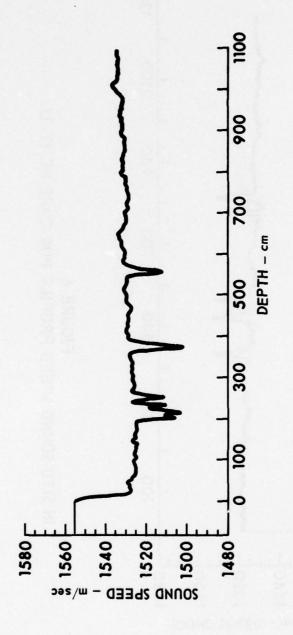
(AFTER TUCHOLKE, 1976)

FIGURE 5
IN SITU SOUND SPEED PROFILE FOR CORE RC 19-15
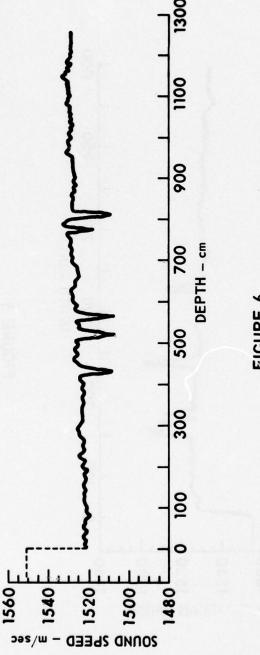
FIGURE 6

IN SITU SOUND SPEED PROFILE FOR CORE RC 19 - 17
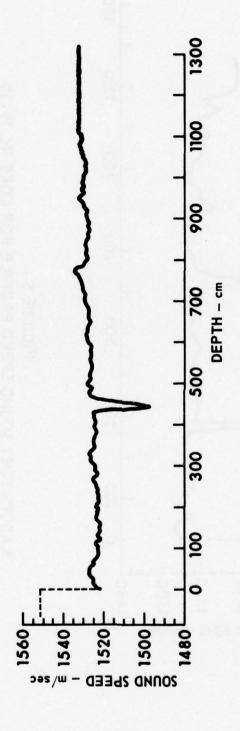
FIGURE 7

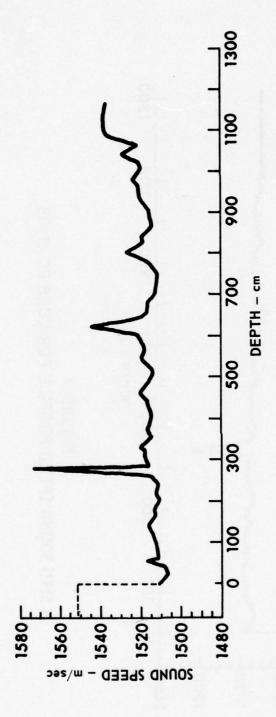IN SITU SOUND SPEED PROFILE FOR CORE RC 19-18

FIGURE 8

LABORATORY SOUND SPEED PROFILE FOR CORE RC 19-15
(AFTER TUCHOLKE, 1976)
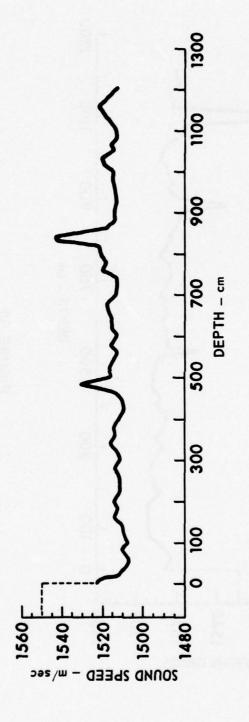
FIGURE 9

LABORATORY SOUND SPEED PROFILE FOR CORE RC 19 - 17
(AFTER TUCHOLKE, 1976)
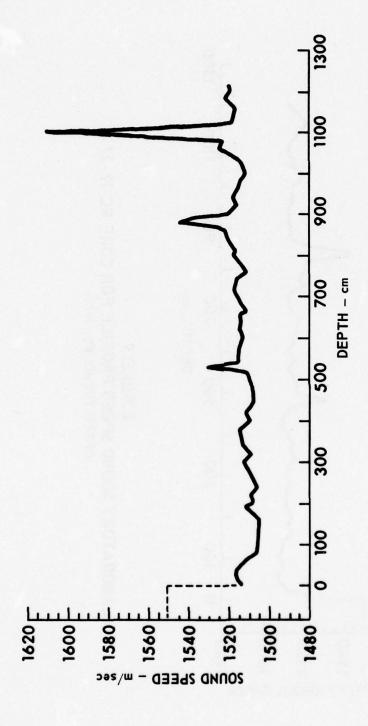
FIGURE 10

LABORATORY SOUND SPEED PROFILE FOR CORE RC 19 - 18

(AFTER TUCHOLKE, 1976)

16

laboratory sound speed profiles made aboard ship. These three cores were made about 1 mile apart and so are quite similar. The dotted portion of the profiles in Figs. 6 and 7 shows equivalent water sound speeds; these water sound speeds were missing from the in situ data for these cores.

Table II shows some of the acoustic parameters calculated for six of the cores. The sound speed ratio is the ratio of sound speed in the top of the sediment to the sound speed in the overlying water. In the case where there is a data dropout at the beginning of the profile, a straight line fit was made to the linear portion of the curve and the sound speed indicated by this line at zero depth in the profile was taken as the surface sound speed. This straight line fit is shown as a dotted line in Fig. 2. Sound speed gradients were also calculated in the same manner using the slope of a straight line fitted to the profile. For the laboratory data, least square fits were calculated for tabulated data points along the profile.

The profilometer was again used 23 June - 4 July 1976 to measure sound speed profiles in situ during a field trip conducted by The University of Texas Marine Science Institute (MSI) Geophysics Laboratory in the Gulf of Mexico near Panama City, Florida. The coring was done from R/V IDA GREEN operated by MSI. Seventy-seven cores were made at 71 locations of which at least 60 in situ sound speed profiles were successfully made. Figure 11 shows a plot of core locations for the cruise. In the shallow water near the coast the cores were mostly sand and shell with penetrations on the order of 1 m. In deeper water penetration increased to as much as 13 m at locations with high clastic content.

A sample of the type of sound speed profiles made on the IG-19 cruise is shown in Figs. 12 through 14. These three sound speed profiles were made for cores 73, 74, and 75 on a line which included water depths

17

TABLE II

TABLE OF ACOUSTIC PARAMETERS FOR SIX ATLANTIC CORES

Core ID	Core Location	In situ		Laboratory	
		Sound Speed Ratio C_s/C_w	Sound Speed Gradient sec^{-1}	Sound Speed Ratio C_s/C_w	Sound Speed Gradient sec^{-1}
RC19-14	Southwest Bermuda Rise	0.990	0.50	0.97	1.10
RC19-15	West Antilles Outer Ridge	0.983	0.97	0.97	1.43
RC19-17	West Antilles Outer Ridge	0.981	0.85	0.98	0.40
RC19-18	West Atnilles Outer Ridge	0.982	0.90	0.98	0.95
RC19-20	Nares Abyssal Plain	0.990	1.07	0.97	0.42
RC19-21	Nares Abyssal Plain	0.990	0.52	0.97	1.08
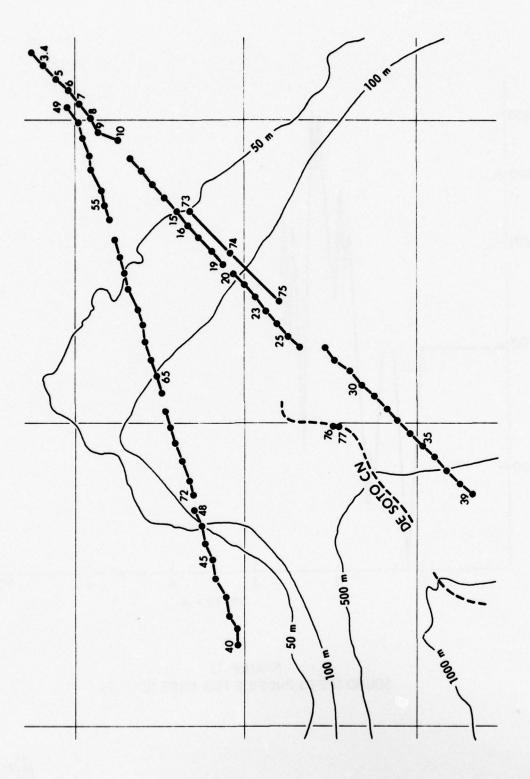
FIGURE 11

CORE LOCATION FOR R/V IDA GREEN CRUISE IG-19
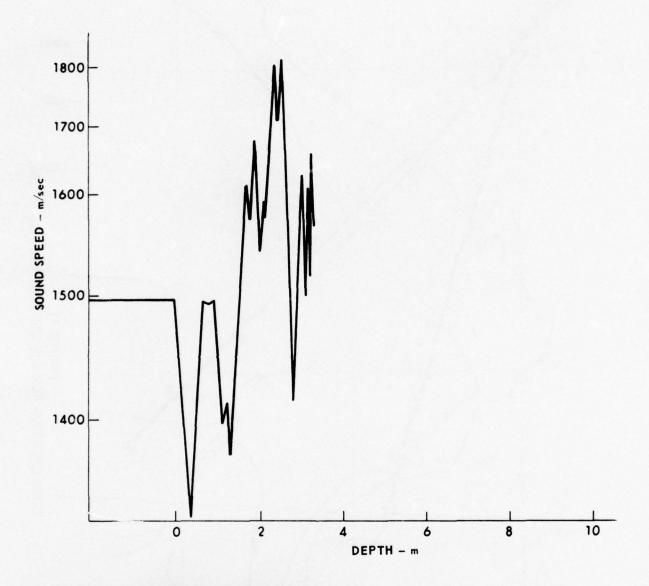
FIGURE 12
SOUND SPEED PROFILE FOR CORE IG 19 -73
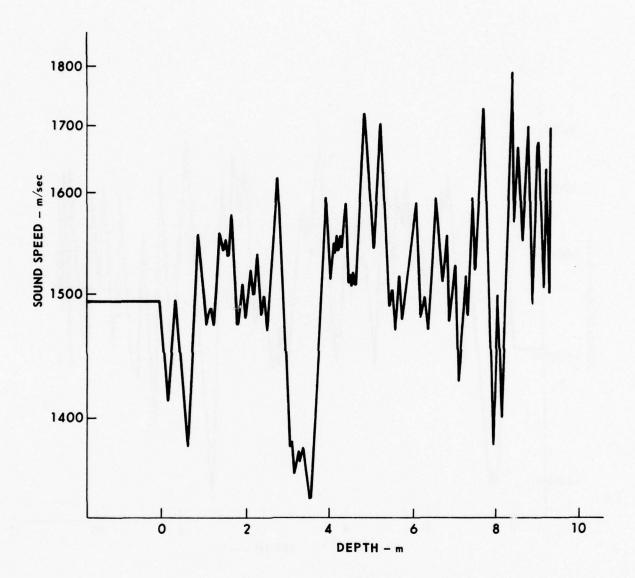
FIGURE 13
SOUND SPEED PROFILE FOR CORE IG 19-74

21
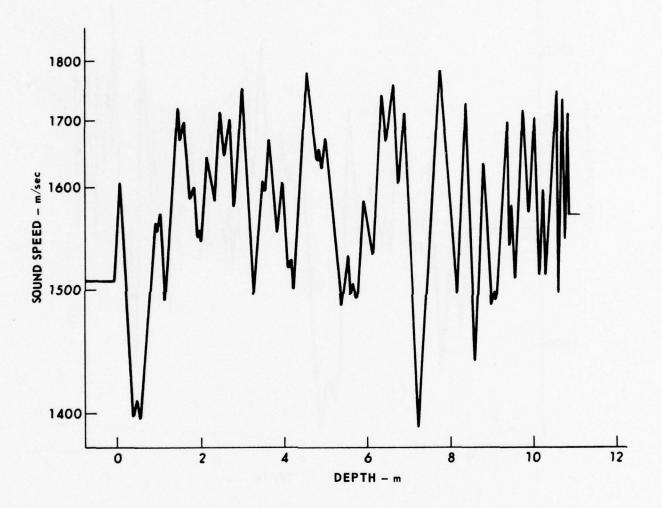
FIGURE 14
SOUND SPEED PROFILE FOR CORE IG 19-75

22

from 50 m to 150 m (see Fig. 11). Core 73 contained a much higher percentage of sand than cores 74 and 75, which explains the shallower penetration, about 3 m, as compared to about 9 m for cores 74 and 75. All three cores show a sound speed higher than that of the overlying water; this high sound speed is the result of the large percentage of sand and the consequent low porosity. All the profiles also show data dropouts, of the type described previously, which show up as low sound speed layers. The dropouts are especially severe during initial penetration and are probably caused by the initial hard impact of the core on the sandy sediment.

A field trip with the profilometer was conducted with WHOI aboard C/S LONGLINES 6-15 October 1976 in the North Pacific. No profiles were made due to the loss of the profilometer when one of the giant corers was not retrieved.

In summary ARL:UT personnel took the profilometer on four field trips to various parts of the world. Of the four trips, data were successfully recorded on two for a total of about 66 in situ sound profiles.

III. SHEAR WAVE TRANSDUCER

The present configuration of the ARL:UT profilometer allows only
the measurement of compressional wave parameters on ocean sediments.
A sediment will also support shear wave propagation due to the rigid
framework developed from grain-to-grain contact. The propagation speeds
of compressional and shear waves are described by the following equations,
where C_p is compressional wave speed, C_s is shear wave speed, k is bulk
modulus, G is shear modulus, and ρ is bulk density.

$$C_p = \sqrt{\frac{k + \frac{4}{3} G}{\rho}} \quad , \tag{1}$$

$$C_s = \sqrt{\frac{G}{\rho}} \quad . \tag{2}$$

Thus the elastic moduli of a sediment can be determined by a
measurement of the three parameters of C_p, C_s, and ρ. If the visco-
elastic parameters of a sediment are required, the measurement of
compressional and shear wave attenuation is also needed.

Since the same argument can be made for the measurement of shear
wave parameters in situ as for compressional wave measurements (i.e.,
disturbance, temperature, and pressure changes, etc.), ARL:UT started
about three years ago on a program to develop small, rugged transducers
to generate and detect shear waves. These transducer elements were to
be used in a profilometer system, as the compressional transducers are.

In the initial portion of the shear wave studies, optimum
configurations of conventional shear plate ceramic transducers were
devised and tested. Sensitivity was only sufficient to allow laboratory

measurements of shear waves in sediments of dynamic shear moduli on the order of 10^7 dynes/cm^2. Since most in situ ocean sediments have moduli well below this value, further improvement in sensitivity was required. Most of the low sensitivity was due to poor coupling (there is a large impedance mismatch between the very stiff, high wave speed ceramic and the highly compliant, low speed sediment) and to the high resonance frequency of the transducer necessitating operation at frequencies where attenuation is high.

A significant improvement in sensitivity resulted when a transducer element using ceramic bender elements was constructed and tested. A ceramic bender combines the requisite properties of high compliance and low resonance frequency in a small size. The preliminary work using the bender element has been reported (Shirley and Anderson, 1975).

The past year's development of the shear wave transducer has concentrated on redesigning the elements that were initially constructed to operate at atmospheric pressure to operate at the pressures encountered at the ocean bottom.

Figure 15 shows the construction of the initial type of bender transducer. From three to six bender elements were formed into an array with compliant spacers cemented between the individual elements to hold them together, yet allow each element to bend independently.

A transducer array configuration was chosen that would provide a larger coupling area and more motional force to the radiating face. However, the compliance of the spacers is very important since any restriction of the bending of the element degrades performance and results in loss of sensitivity. Both corprene (a cork-neoprene compound) and light cardboard have been successfully used in transducers for laboratory use. Once pressure has increased over a few hundred kilopascal, both these materials would be compressed and would become rigid. The result would be low sensitivity and possible failure of the transducer from breakage.
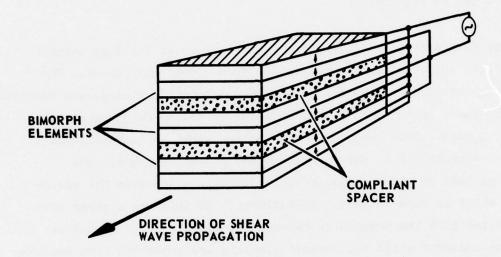
26

BIMORPH ELEMENTS

COMPLIANT SPACER

DIRECTION OF SHEAR WAVE PROPAGATION

FIGURE 15
SHEAR WAVE TRANSDUCER
UTILIZING BENDER ELEMENTS

27

One alternative to the above design is to use a single element instead of an array of elements to generate the shear wave. There is some loss of motional force, but the fact that no spacers are required make this a reasonable approach.

Another approach would be to build an array using a rigid spacer to connect the ends of the benders together, leaving the center spacing open. This approach would increase the complexity, but could possibly increase the sensitivity.

The next aspect of designing a shear transducer for high ambient pressure is the mounting and protection from a wet environment. The laboratory version of the shear transducer not only has compliant spacers but also has a layer of compliant material on all surfaces except the radiating face. This compliant covering isolates the bender elements from the encapsulant to ensure free motion of each element. The radiating face of the transducer is in direct contact with the encapsulant which in turn contacts the sediment. In this way a shear wave is radiated from the transducer through the plastic "window" and on into the sediment while the ceramic elements are protected from becoming wet and shorted.

For high ambient pressure, the compliant covering on the transducer elements must be eliminated. The single element can be potted directly in the encapsulant and, if the encapsulant is flexible enough, the element can still bend and generate or detect a shear wave. Transducers have been constructed in this manner using various flexible encapsulants such as Scotchcast 221, PRC 1527, and RTV rubber. In the best of these transducers, signal levels across an equivalent sediment path were reduced 30 dB from the levels obtained by the laboratory type transducer; this level is not sufficient for work in clays and muds.

Another approach is illustrated in Fig. 16. The single element is held in position by rigidly attaching it to the back of the metal housing.

28

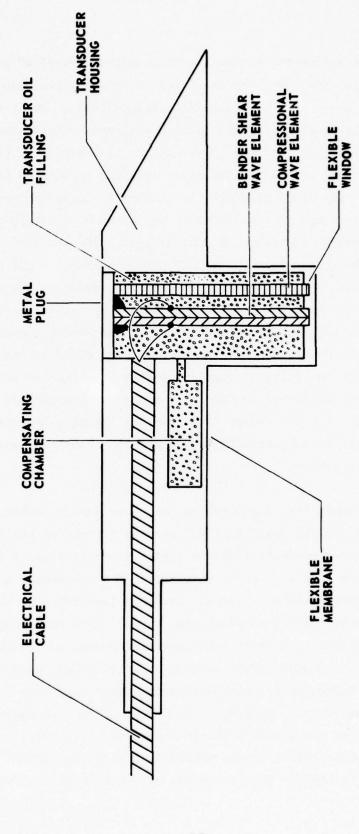FIGURE 16
SCHEMATIC DRAWING OF COMPOSITE PROFILOMETER TRANSDUCER

TRANSDUCER OIL FILLING

TRANSDUCER HOUSING

BENDER SHEAR WAVE ELEMENT

COMPRESSIONAL WAVE ELEMENT

FLEXIBLE WINDOW

METAL PLUG

COMPENSATING CHAMBER

ELECTRICAL CABLE

FLEXIBLE MEMBRANE

The other end of the bender element is attached to a "window" of flexible plastic which protects the interior of the transducer from seawater and also allows the shear wave to couple into the sediment. The interior of the transducer housing is filled with a dielectric fluid such as silicone transducer oil, and this fluid allows free motion of the bender even at high ambient pressure. The major drawback to such an arrangement is the fact that the fluid filling will be compressed by an increase in pressure and a decrease in temperature. For silicone oil this would amount to a reduction in volume of 3.6% at 3.45×10^{4} kPa and 2.5% for for a temperature change from 25° to 0°C. In a transducer the size appropriate to the profilometer (1.9 cm diam x 25 cm long) the window would be pushed in about 1.7 mm. This amount of motion of the window could possibly either push the element through the window and expose it to the water or it could fracture the element. To eliminate this problem, the transducer can be pressure compensated by connecting the interior of the transducer to another chamber with a thin window exposed to the ambient pressure. All the change in volume will be made by motion of the membrane over the compensating volume and thus eliminate any motion of the transducer window.

A set of transducers incorporating the above design features have been constructed and are awaiting field testing to confirm their usefulness. Laboratory tests indicate that the sensitivity of these transducers is comparable to those constructed for laboratory use. In addition, a ceramic transducer element has been included that can be used to generate and detect compressional waves. This compressional wave element consists of a ceramic element with dimensions on the same order as that of the bender (0.64 cm wide x 2.5 cm long), except that this element is driven in a length-extensional mode such that it is resonant at about 70 kHz. This type of element is an experimental attempt to overcome one of the problems discussed previously, when coring high speed turbidite layers embedded in soft clays where the layer thickness is smaller than the width of the transducer element,

multipath phase interference occurs and causes data dropouts and consequently an incomplete profile. The much thinner compressional wave transducer element in the new design should be able to detect a finer lithologic structure than was possible before.

31

IV.   SHEAR WAVE MEASUREMENTS

Measurements of shear and compressional wave parameters of laboratory type sediments have been made as a necessary part of the transducer development. Measurements in the laboratory can demonstrate relative merit of particular transducer designs as well as provide new data. The laboratory measurements part of the program has concentrated during the past contract year on determining the acoustic parameters of various sands.

Three types of sand were used for testing (1) a coarse riverbed sand with widely varying grain size, consisting mostly of quartz and feldspar grains, referred to as red sand, (2) a medium fine white beach sand from Panama City, Florida, having a relatively narrow range of grain sizes and consisting mostly of semirounded quartz grains, referred to as PC sand, and (3) a fine sandblasting sand of smooth quartz grains with a narrow size range, termed SB sand. Table III shows the grain size analysis for these sands.

For the acoustic measurements, each of the sands was prepared by saturating it with water. The water-sand mixture was then placed in a vacuum chamber to remove any entrained air. The mixture was then placed in a 15.2 x 30.5 x 15.2 cm aluminum tank with shear wave and compressional wave transducers inserted at measured spacing in the sand. To obtain a range of porosities for each of the sand types, the sands were progressively compacted by vibrating the tank with an electromagnetic vibrator. After each interval of vibration, shear and compressional wave speeds were measured as well as shear wave amplitude. The measurements were repeated for several different spacings of the transducers. At each spacing, the shear measurements were made at center frequencies of 300, 600, 1000, and 1600 Hz in an attempt to detect changes in speed or

TABLE III

Grain Size (φ Units)	Red Sand	PC Sand	SB Sand
-1 to -1/2	0.45%	0	0
-1/2 to 0	1.14	0	0
0 to 1/2	17.95	0	0
1/2 to 1	13.75	0.43%	0.06%
1 to 1 1/2	22.74	47.02	0.22
1 1/2 to 2	25.12	41.36	3.00
2 to 2 1/2	12.07	10.59	36.20
2 1/2 to 3	5.13	0.58	49.79
3 to 3 1/2	1.49	0	8.74
3/2 to 4	0.14	0	1.95
<4	0	0	0.04

34

attenuation with frequency. Porosity was determined at each level of compaction by measuring the volumetric change of the sand fraction of the sand-water mixture.

Figure 17 displays the shear wave speed versus porosity for the three sands while Fig. 18 shows the compressional wave speed. A least squares fit is drawn as a solid line for each of the curves. No change in shear wave speed with frequency was detected.

Attenuation values were calculated from the amplitude measurements at different spacing, but the large amount of scatter in the data prevents any conclusion as to frequency dependence of the attenuation. The attenuation coefficient (α) versus frequency for red sand is plotted in Fig. 19. The solid line is a line plotted for $\alpha = CF^1$, where C is an arbitrary constant. The scatter in the data is due to interference from reflections in the small tank, especially at the lower frequencies.

With the shear and compressional wave speed data and the porosity available, the bulk modulus (k), shear modulus (G), and frame bulk modulus (k_f) were then calculated. Figures 20 through 22 show these three moduli versus porosity for the three sands. Figure 23 shows the frame bulk modulus also plotted with data from other sediment types and sources (Hamilton 1971). The black dots are data points with a least squares fit line provided by Hamilton. The sand data are drawn in with X's at the data points. Only the fine sand blasting sand deviates appreciably from Hamilton's curve.

FIGURE 17
SHEAR WAVE SPEED versus POROSITY
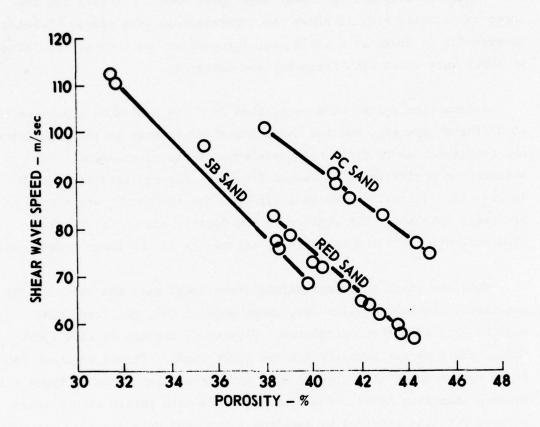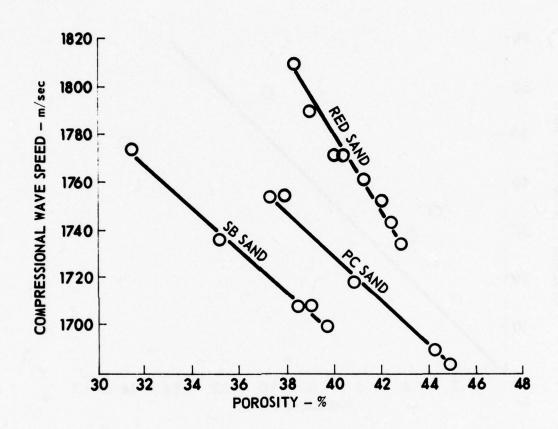
FIGURE 18
COMPRESSIONAL WAVE SPEED versus POROSITY
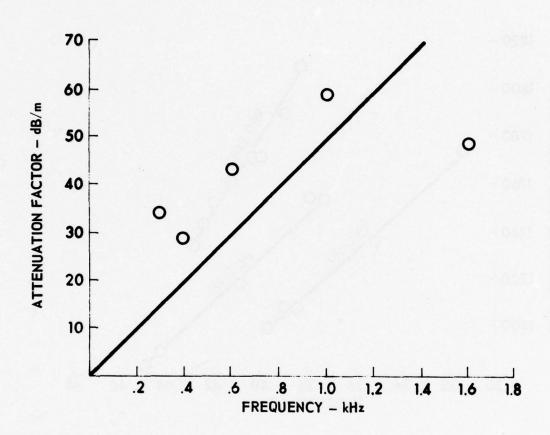
FIGURE 19
SHEAR WAVE ATTENUATION versus FREQUENCY

38
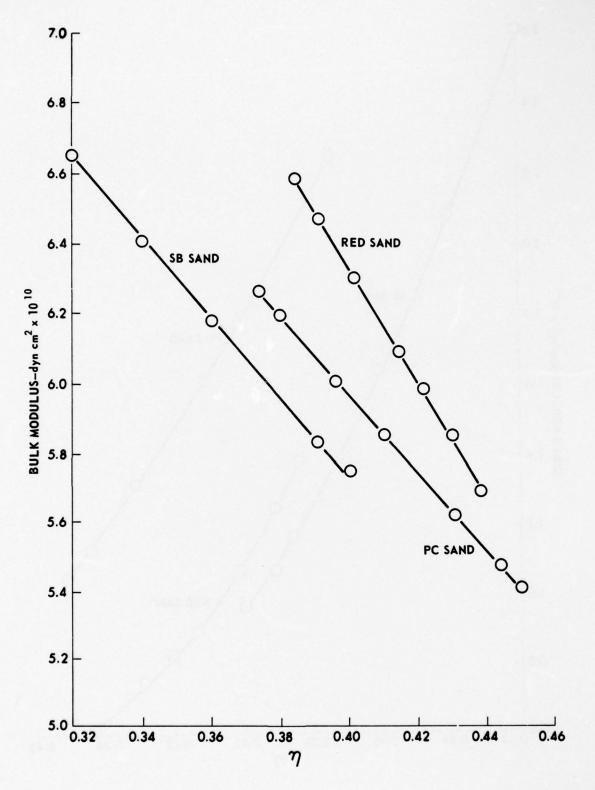
FIGURE 20
BULK MODULUS VERSUS POROSITY FOR THREE SANDS

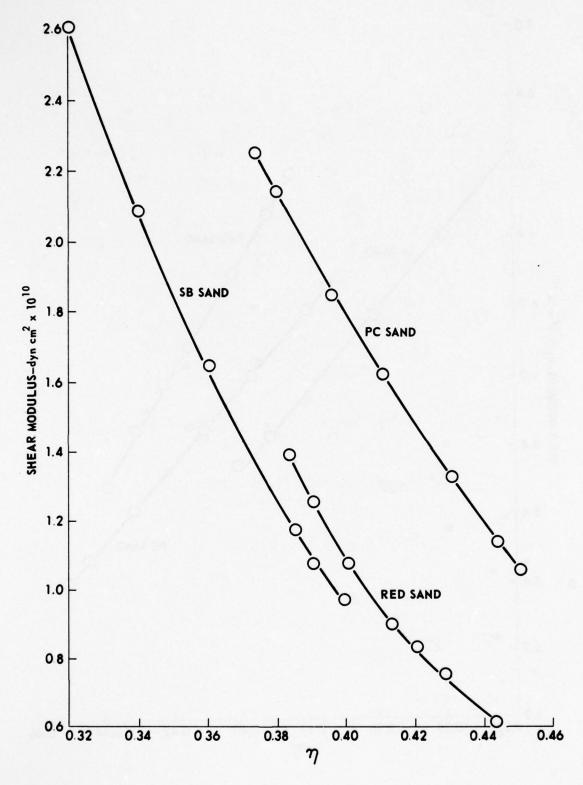**FIGURE 21**
SHEAR MODULUS VERSUS POROSITY FOR THREE SANDS

40
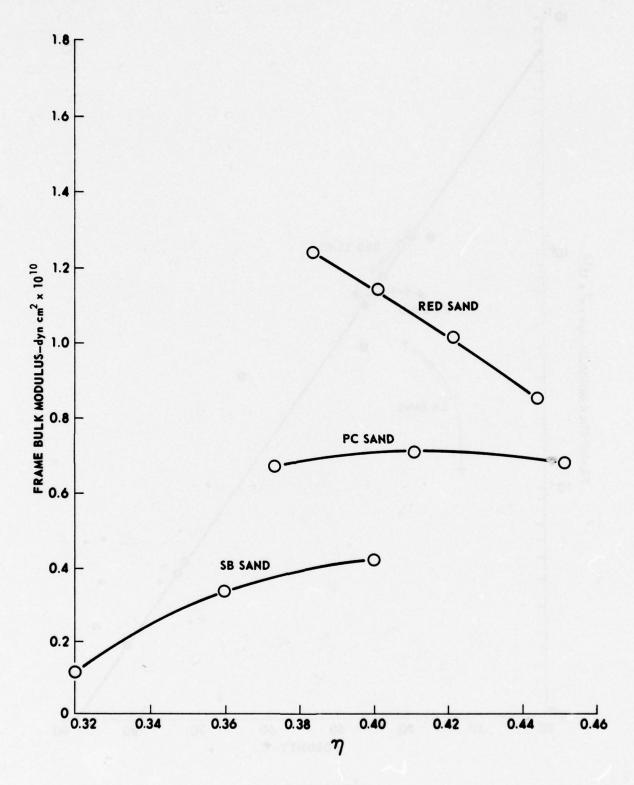
FIGURE 22
FRAME BULK MODULUS VERSUS POROSITY FOR THREE SANDS

41
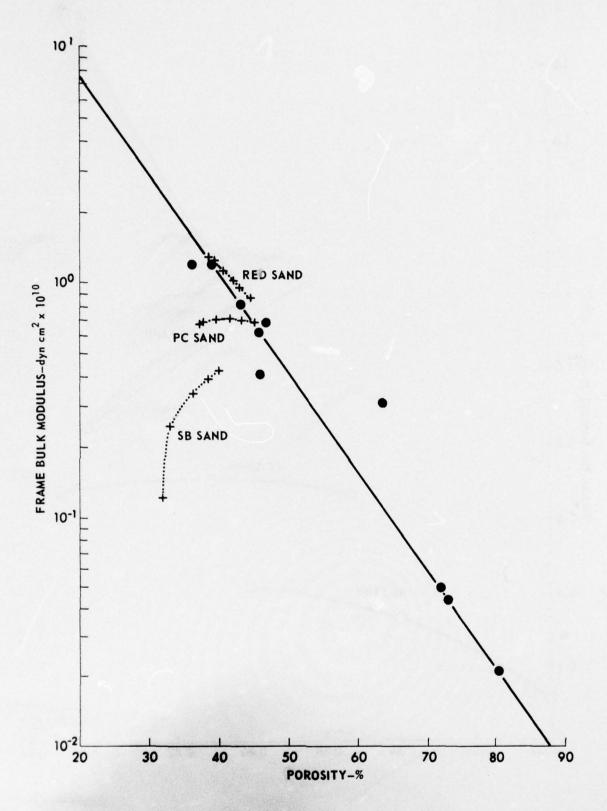
FIGURE 23
SEDIMENT FRAME BULK MODULUS VERSUS POROSITY
(AFTER HAMILTON 1971)

V. ACOUSTIC IMPEDANCE

If the bulk density (ρ) of a sediment is measured concurrently
with compressional wave speed and attenuation and shear wave speed and
attenuation, the dynamic physical parameters can be calculated. A
common method of measuring the density of marine sediments is to determine
volume and weight of a small sample removed from a core aboard ship.
The sample is subject to disturbance and changes of temperature and
pressure from the in situ conditions. Also, since the weight of a
small sample cannot be accurately determined aboard ship, the sample is
subject to further disturbance and drying during transfer back to a shore
based lab. All these factors tend to degrade the accuracy of such a bulk
density measurement.

Another method of bulk density measurement has been proposed and
is under development at ARL:UT. This method relies on a measurement of
the acoustic impedance (ρC_p) of the sediment with a concurrent measure-
ment of compressional wave speed (C_p). One value of this method is the
fact that the measurement can be made in situ with profilometer type
equipment.

If one considers the radiation loading on a driven transducer
element immersed in some medium with characteristic acoustic impedance
$\rho_o C_o$, then the radiation load R_R is given by

$$R_R = \frac{Z_R}{\alpha^2} \quad ,$$

where Z_R is the mechanical radiation impedance and α is the mechanical
to electrical transformation factor. For a large ratio of radiation

area A to wavelength λ, the equation for R_R reduces to

$$R_R = \frac{2A\rho_o C_o}{\alpha^2} \quad .$$

The above relationship shows that a measurement of R_R, which can be measured electrically, is a direct measurement of $\rho_o C_o$ since A and α are constants. If C_o is measured concurrently, ρ_o can be calculated from the acoustic impedance measurement.

A transducer was designed and built to test the feasibility of measuring ρC electrically. Figure 24 shows a cross sectional drawing of the transducer that was used in the preliminary testing. Styrofoam was chosen as the backing material to approximate as closely as possible a pressure release surface at the back and sides of the ceramic element. Thus, to all intents, the only loading on the element is the acoustic radiation load of the medium in contact with the thin plastic window. The purpose of the window is to protect the ceramic element from moisture.

The element was composed of a lead-zirconate titanate (PZT-5) ceramic and was 1.59 cm long x 1.27 cm wide x 0.40 cm thick. It was polarized and driven in the thickness dimension. Figure 25 shows an admittance plot of the transducer measured with an air load. The center of the admittance circle is a short distance above the G-axis. This distance represents the change in B due to cable capacitance and the clamped capacitance of the element. Addition of a 1 mH inductor across the driven end of the cable brought the center point down onto the G-axis, where B=0 is the resonance frequency of the element with an air load. The resonance frequency for this mode was 108.975 kHz.

The transducer was mounted through the wall of a small aluminum tank into which the various media could be introduced for testing. Due to interference from standing waves in the tank, a short (10 msec) tone
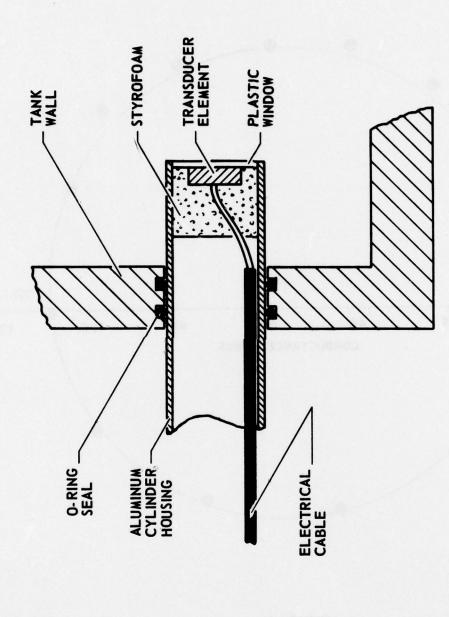
44

FIGURE 24
ACOUSTIC IMPEDANCE TRANSDUCER

TANK
WALL

STYROFOAM

TRANSDUCER
ELEMENT

PLASTIC
WINDOW

O-RING
SEAL

ALUMINUM
CYLINDER
HOUSING

ELECTRICAL
CABLE
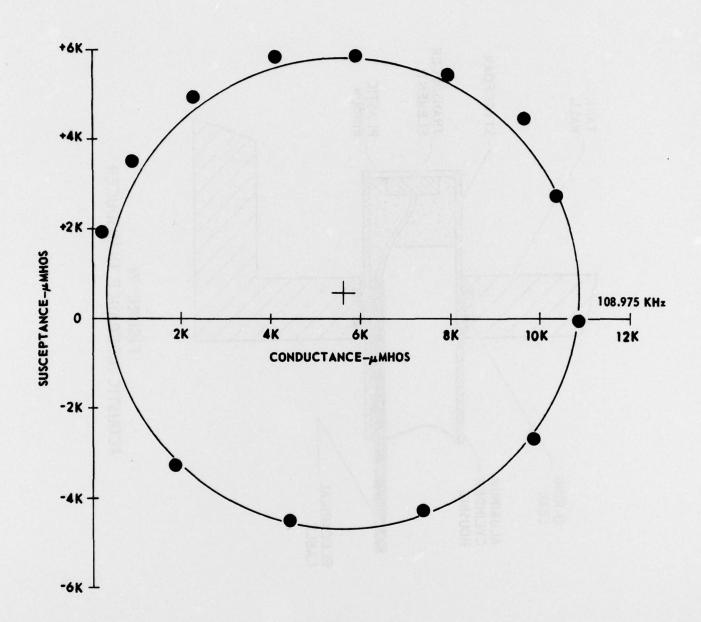
FIGURE 25
ADMITTANCE PLOT IN AIR OF ACOUSTIC IMPEDANCE TRANSDUCER

burst was used for testing. A 10 W power amplifier was used to drive
the transducer in series with a 10 Ω current sensing resistor. The
waveform across the transducer and the waveform across the resistor
were displayed on an oscilloscope to provide a measure of the voltage
across the transducer and the current through it. Measurements were
made at resonance (i.e., when the current and voltage waveforms were
totally in phase) with the driving voltage set at a constant 30 V
peak-to-peak. Electrical impedance of the transducer was calculated
from the voltage and current values. Independent measurements of
density and sound speed were made for each different sediment that was
used.

Figure 26 shows a plot of the electrical impedance for the
transducer versus the acoustic impedance for a number of different
sediments plus values for water and air. As expected, there is a linear
relationship between the electrical parameters of the transducer and the
mechanical parameters of the sediments. The measurement also shows that
there is good sensitivity of the electrical measurement to the mechanical
values. Each set of points in Fig. 26 is labeled with the sediment type.
The straight line in the figure is a least squares fit to the data points.
The scatter in the data is felt to be due more to inaccuracies in the
independent measurement of bulk density. This is a difficult parameter
to measure accurately, especially in sands, because of the problem of
obtaining an accurate undisturbed volume of the material.

It was recognized that changes in temperature and pressure encountered
in the normal ocean environment would affect the measurements made with
a ceramic element. For this reason, measurements were made at tempera-
tures between 52° and 6°C of the electrical impedance of the transducer
with pure water as the loading medium. Density and sound speeds of pure
water are known to good accuracies so that the actual measurements with
the transducer can be compared to the expected values calculated using
the least squares fit from Fig. 26.
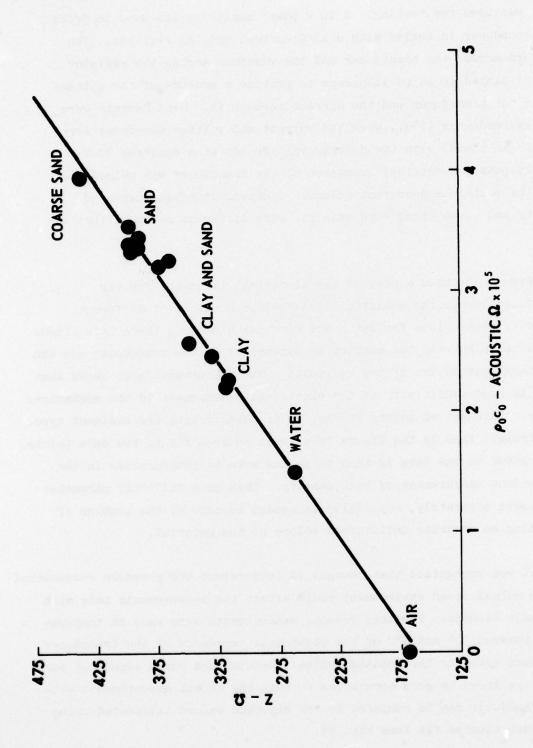
FIGURE 26

PLOT OF ELECTRICAL IMPEDANCE versus
ACOUSTIC IMPEDANCE FOR A TRANSDUCER

Figure 27 shows the results of the temperature measurements. The straight line shows the calculated values of electrical impedance derived from the least squares fit of Fig. 26 and the known values of ρC for water at various temperatures. Below about 30°C, there is good agreement between the measured data and the calculated values, but above 30°C the measured data shows a marked difference from the expected value. However, in the real ocean environment temperatures in this range are seldom encountered--especially in bottom sediments at the depth to which a corer can penetrate.

The dependence of acoustic impedance upon ambient pressure has not as yet been determined. Since the present transducer configuration is only usable at atmospheric pressure, tests at pressures encountered in the ocean must await design of a transducer that can withstand high ambient pressure.
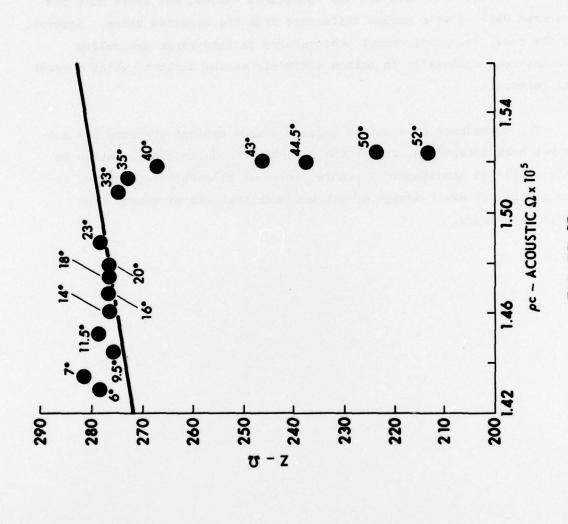
FIGURE 27

TEMPERATURE DEPENDANCE OF ACOUSTIC IMPEDANCE MEASUREMENTS

50

VI. CONCLUSIONS

Profilometer

The existing compressional wave profilometer design has been used during the past contract year on four major field trips with four different oceanographic institutions. A total of 66 sound speed profiles were made. The existing instrument was lost on the final field trip, so that a new unit had to be constructed.

Shear Wave Transducer

Work has continued on the development of shear wave transducers for use in deep ocean sediments. Prototypes have been built and await testing. Laboratory measurements have been made on three sands at a wide range of frequencies; however, the scatter in the data resulting from reflections in the test tank obscured the frequency dependence of attenuation.

Acoustic Impedance

A method has been developed to measure the acoustic impedance of a sediment by measuring the electrical impedance of a transducer in contact with the sediment. Laboratory work conducted during the past year has revealed that a linear relation exists between the electrical impedance and the acoustic impedance. The measurements were shown to be independent of temperature below 30°C. Further work is required to design a transducer to operate at sea bottom pressures and to determine the pressure dependence of measurements with such a transducer.

23 August 1977

DISTRIBUTION LIST FOR
ARL-TR-77-46
UNDER CONTRACT N00014-76-C-0117
UNCLASSIFIED

Copy No.

	Commanding Officer Naval Ocean Research and Development Activity NSTL Station, MS 39529
1	Attn: R. R. Goodman (Code 110)
2	R. D. Gaul (Code 600)
3	A. L. Anderson (Code 320)
4	Samuel Marshall (Code 340)
5	Herbert Eppert (Code 360)
6	Thomas Pyle (Code 430)
7	Hugo Bezdek (Code 460)
8	G. J. Ranes (Code 500)
9	J. Paquin (Code 600)
10	K. V. Mackenzie (Code 340)
11	James Matthews (Code 362)

	Commanding Officer Naval Electronic Systems Command Department of the Navy Washington, DC 20630
12	Attn: J. Sinsky (Code 320)
13	W. Kamminga (Code 320)
14	Jesse Reeves (Code PME 124-34)

	Commander Naval Sea Systems Command Department of the Navy Washington, DC 20362
15	Attn: A. P. Franceschetti

	Commanding Officer Office of Naval Research Arlington, VA 22217
16	Attn: J. B. Hersey (Code 102-OS)
17	Al Sykes

	Hawaii Institute of Geophysics The University of Hawaii 2525 Correa Road Honolulu, HI 96822
18	Attn: Dr. G. Sutton

53

Copy No.

	Commander
	Naval Ocean Systems Center
	Department of the Navy
	San Diego, CA 92132
19	Attn: M. A. Pedersen (Code 307)
20	R. R. Gardner (Code 40)
21	Edwin L. Hamilton
22	Homer P. Bucker (Code 409)
23	G. Mohnkern
24	John Northrop

Director
Naval Research Laboratory
Department of the Navy
Washington, DC 20375
25 Attn: (Code 2627)
26   O. Diachok
27   Library (Code 2620)
28   Library (Code 2000)

Naval Oceanographic Office
Department of the Navy
Washington, DC 20373
29 Attn: W. H. Geddes

Chief of Naval Operations
Department of the Navy
Washington, DC 20350
30 Attn: R. S. Winokur CNO (OP-95E1)

Commander
Naval Air Development Center
Department of the Navy
Warminster, PA 18974
31 Attn: C. L. Bartberger

Commander
New London Laboratory
Naval Underwater Systems Center
Department of the Navy
New London, CT 06320
32 Attn: P. Herstein

The Scripps Institution of Oceanography
The University of California/San Diego
San Diego, CA 92152
33 Attn: Peter Lonsdale

Copy No.

	Commanding Officer
	Naval Coastal Systems Laboratory
	Panama City, FL 32401
34	Attn: E. G. McLeroy, Jr.
35	Bill Tolbert

	Superintendent
	Naval Postgraduate School
	Monterey, CA 93940
36	Attn: H. Medwin

	Woods Hole Oceanographic Institution
	Woods Hole, MA 02543
37	Attn: Dr. Charles Hollister
38	Dr. Alan Driscoll
39	Dr. Earl Hayes

	Department of Geological Oceanography
	Texas A&M University
	College Station, TX 77840
40	Attn: Dr. William R. Bryant

	Underwater Systems, Inc.
	3121 Georgia Avenue
	Silver Spring, MD 20910
41	Attn: Marvin S. Weinstein

	Geophysics Laboratory
	Marine Science Institute
	The University of Texas
	700 The Strand
	Galveston, TX 77550
42	Attn: J. Worzel
43	E. W. Beherns

	TRACOR, Inc.
	1601 Research Boulevard
	Rockville, MD 20850
44	Attn: R. J. Urick

	The Catholic University of America
	6220 Michigan Avenue, NE
	Washington, DC 20017
45	Attn: H. M. Uberall

Copy No.

	Lamont-Doherty Geological Observatory Palisades, NY 10964
46	Attn: G. Bryan
47	W. J. Ludwig
48	B. Tucholke

	Department of Civil and Ocean Engineering The University of Rhode Island Kingston, RI 02881
49	Attn: Dr. Armand J. Silva

	Commanding Officer and Director
50 - 59	Defense Documentation Center Defense Services Administration Cameron Station, Building 5 5010 Duke Street Alexandria, VA 22314

	University College of North Wales Marine Science Laboratories Menai Bridge Anglesey, North Wales
60	Attn: D. Taylor Smith

	Director SACLANT ASW Research Centre LeSpezia, Italy
61	Attn: T. Akal

	The University of Auckland Physics Department Auckland, New Zealand
62	Attn: Alick Kibblewhite

63	Defense Research Establishment Pacific CF Dockyard Victoria, B. C., Canada

64	Defense Research Establishment Atlantic Grove Street Dartmouth, N. S., Canada

	University College of Swansea Department of Geology and Oceanography Singleton Park Swansea SA2 8PP, United Kingdom
65	Attn: Peter Schultheiss

Copy No.

	Department of Civil Engineering The University of Texas at Austin Austin, TX 78712
66	Attn: K. Stokoe
	The University of Texas Marine Science Institute P.O. Box 7999 University Station Austin, TX 78712
67	Attn: Dr. C. A. Burke
68	Office of Naval Research Resident Representative Room 582, Federal Building Austin, TX 78701
69	Environmental Sciences Division, ARL:UT
70	Garland R. Barnard, ARL:UT
71	David T. Blackstock, ARL:UT
72	Glen E. Ellis, ARL:UT
73	Karl C. Focke, ARL:UT
74	Harlan G. Frey, ARL:UT
75	Loyd D. Hampton, ARL:UT
76	Kenneth E. Hawker, ARL:UT
77	C. W. Horton, ARL:UT
78	Chester M. McKinney, ARL:UT
79	Thomas G. Muir, ARL:UT
80	Donald J. Shirley, ARL:UT
81	Reuben H. Wallace, ARL:UT
82	Charles L. Wood, ARL:UT
83	Library, ARL:UT
84 - 93	Reserve, ARL:UT